Manuscript

Click here to download Manuscript Correlated selection on amino acid ... 7.2.docx

Click here to view linked References

Correlated selection on amino acid deletion and replacement in mammalian protein sequences

Yichen Zheng[1,2], Dan Graur [2], Ricardo B. R. Azevedo[2]

1 Institute of Genetics, University of Cologne, Cologne, NRW 50674, Germany

2 Department of Biology and Biochemistry, University of Houston, Texas 77204-5001, USA

Email addresses: Yichen Zheng: yzheng2@uni-koeln.de; Dan Graur: dgraur@uh.edu; Ricardo B. R. Azevedo: razevedo@uh.edu

Corresponding author: Yichen Zheng (+49-221-470-1564)

Abstract

A low ratio of nonsynonymous and synonymous substitution rates (dN/dS) at a codon is a sign of functional constraint caused by purifying selection. Intuitively, the functional constraint would also be expected to prevent such codon from being deleted. Oddly, to the best of our knowledge, the correlation between the rates of deletion and substitution has never actually been measured. Here, we use 8,595 protein coding-region sequences from 9 mammalian species to examine the relationship between deletion rate and dN/dS. We found significant positive correlations at both the level of sites and genes. We compared our data against controls consisting of simulated coding sequences evolving along identical phylogenetic trees. A much weaker correlation were found in the corresponding simulated sequences, which is probably caused by alignment errors. In the real data, the correlations in the real data cannot be explained by alignment errors. Separate investigations on nonsynonymous (dN) and synonymous (dS) substitution rates indicate that the correlation is most likely due to a similarity in patterns of selection rather than mutation rates.

Keywords

Mammals, Protein-coding genes, dN/dS, Codon deletion, Purifying selection

Introduction

The functional constraint on a genomic region is defined by its sensitivity to mutations, that is, the proportion of mutations that negatively affect its function (Graur 2016). Genomic regions subject to strong functional constraints are

expected to perform important functions and to evolve relatively slowly. Mutations can take many forms, including nucleotide substitutions, insertions, and deletions (indels); as a result, functional constraint can be defined separately with respect to each type of mutation. One might expect functional constraints with respect to nucleotide substitutions and indels to be correlated — if the function of a genomic region can be disrupted by a substitution it can probably also be disrupted by an indel. However, this is not necessarily the case. For example, nucleotide substitutions at a fourfold degenerate site in a protein-coding gene may be selectively neutral because the protein product is not affected. If that fourfold degenerate site is deleted, however, it will cause a frameshift that will likely disrupt the function of that protein severely. We have referred to sites that only experience selection when they are deleted as "indifferent DNA" (Graur et al. 2015).

Substitutions have been studied more extensively than deletions, partly because detecting indels is more difficult (Landan and Graur 2009; Nagy et al. 2012). Nevertheless, three studies have attempted to compare the patterns of functional constraint arising from both kinds of mutations. Taylor et al. (2004) identified 1,743 indel events in 1,282 genes (out of a dataset of 8,148 genes) from human-mouse-rat triple alignments. They compared indel rates in genes of different functions (using Gene Ontology), and found that intracellular proteins and enzymes are less likely to have indels. When the indel rate differences were compared with substitution rates (Waterston et al. 2002), a highly similar distribution among categories was found. These results indicate that functional categories that are more "important" to an organism tend to have both reduced amino acid replacement and reduced amino acid loss. One limitation of this study is that it focused on groups of genes rather than on individual genes.

Another study (Miller et al. 2007) used a 28-vertebrate alignment to study coding-sequence conservation. The authors tested the hypothesis that more conserved amino acids are more likely to cause disease when deleted. They analysed the gene encoding the enzyme phenylalanine hydroxylase, loss-of-function of which causes phenylketonuria. The conservation levels of codons involved in disease-causing deletions turned out to be the same as for the gene overall. Miller et al. (2007) concluded that long-term selection against nonsynonymous mutations is consistent with short-term selection (as implied by diseases) against amino acid deletions. One strength of this study was their ability to identify deleterious mutations directly. It is, however, only based on a single gene.

Finally, Chen et al. (2009) studied the ratio of nucleotide substitution to indel rates, across mammalian and bacterial genomes. They interpret the ratio as an indicator of the relative strengths of selection on the two types of mutations. They found that, within coding regions, more conserved genes have higher substitution to indel ratios than less conserved genes. This result suggests that indels (even non-frameshifting ones) are subject to relatively stronger selection than substitutions in conserved genes. However, as the comparison is focused on "which type of mutation is more common", it does not directly help resolving the correlation *between* these two types of changes.

While these aforementioned studies tackled the relationship between purifying selection against nonsynonymous substitutions and purifying selection against deletions, they did not fundamentally answer the question: are the two selection effects correlated across the genome, and what is the extent of this correlation? If the correlation does not exist, one can expect the dN/dS ratio of a codon is independent from its deletion rate. If there is a correlation, the dN/dS ratio would be proportional to the probability of the codon being deleted. dN will also behave

similarly because it is also under selection, while dS would not because it measures neutral substitutions (Nei and Gojobori 1986; Price and Graur 2016). It is also possible that the correlation occurs only at a gene level, i.e., genes with higher dN/dS would have higher deletion rates, but within a gene, the dN/dS and deletion rate of sites are independent. However, selection is not the only evolutionary force that may cause a correlation between substitutions and indels; it is possible that regions with high point mutation rates would also have high indel mutation rates. In this case, we may see that the deletion rate would be correlated to both dN and dS, but not with the dN/dS ratio.

We used mammalian protein-coding sequences and simulated sequences to study the correlation between deletion rates and dN/dS, to understand how similar or different the patterns of the two types of selection are. In addition, we used dN and dS separately to see their correlation with deletion rates, to test our hypothesis on whether or not mutation plays a role. We have found that there is indeed a positive correlation between the rates of deletion and substitution, and it is likely to be caused by selection, rather than mutation.

Results

The deletion and nonsynonymous substitution rates per site are positively correlated

We collected sequences of protein-coding genes from 9 mammalian genomes (Fig. 1), and aligned them with PROBCONS (Do et al. 2005). Simulated alignments were produced along the same phylogenetic tree with realistic parameters derived from the real data (See Supplementary Text). In-frame deletions of length 1-8 amino acids were identified (Fig. 2; see Material and Methods for details); deletion

rate, dN, dS and dN/dS were measured on each codon. Hereafter, we refer to dN, dS, and dN/dS collectively as "substitution measures."

The correlations between deletion rate and the different substitution measures are summarized in Fig. 3. In the "All" dataset the deletion rate is positively correlated with both dN ($\rho = 0.11$) and the dN/dS ratio ($\rho = 0.08$) (Fig. 3A). The corresponding correlations in the simulated data are much lower ($\rho = 0.01$ and 0.03 for dN/dS and dN, respectively; *Z*-test, $P < 0.0001$ in both cases). The signal is even stronger when the true alignments from simulated data are used, indicating the alignment error causes a small inflation of dN/dS and dN estimates (Supplementary Fig. S2). The deletion rate is also positively correlated with dS but the correlation is weaker than for dN ($\rho = 0.04$, Fig. 3A); however, this correlation is significantly stronger in the real data when compared to the simulated data ($P < 0.0001$).

To evaluate the robustness of the patterns summarized in Fig. 3 to uncertainty in the estimates of deletion and substitution rates, we repeated the analysis on the "NC-4+" dataset, containing only sites that have at least one nucleotide substitution and that are present (i.e., not gaps) in at least 4 species. The patterns for dN and dN/dS are essentially unchanged (Fig. 3B). However, the correlation between deletion rate and dS disappears; indeed, the correlation is *higher* in the simulated data than in the real data ($P < 0.0001$). Results for the other four datasets ("4+," "6+," "NC," and "NC-6+") are similar to those for "NC-4+". These results indicate that the correlation between deletion rate and dS is largely driven by sites with low substitution rate and/or uncertain estimates of rates of deletion and substitution. We conclude that rates of deletion and nonsynonymous substitution per site are positively correlated. These results indicate that functional constraints

against amino acid replacement and against amino acid loss are correlated to each other.

Deleted sites show higher rates of nonsynonymous substitution

If the rates of deletion and substitution are positively correlated then sites found to be deleted in at least one taxon would be expected to show a higher rate of substitution than sites that are present in all taxa. Fig. 4 summarizes the results of an analysis testing this prediction. We used Cohen's *D*, a measure of effect size (Cohen 1988). As predicted from the correlation analyses, both dN and dN/dS are much higher in deleted than non-deleted sites. Furthermore, the difference is much higher in real than in simulated data. The differences for dS are also statistically significant, but much smaller in magnitude.

Fig. 5 compares the distributions of dN/dS in deleted and non-deleted sites in the "NC-4+" dataset. In the real data, 63.2% of deleted sites have dN/dS $\geq$ 0.2, while the number is 34.8% for non-deleted sites (Fig. 5A). The difference is negligible in the simulated data (Fig. 5B; 33.6% and 32.2% for deleted and non-deleted sites, respectively). These results confirm rates of deletion and nonsynonymous substitution per site are positively correlated.

The deletion and nonsynonymous substitution rates per gene are positively correlated

To reduce the stochastic effects caused by limited number of mutations on each site, we decided to look at the same correlation at the gene level. We used the same statistical method with gene-averaged deletion rates and substitution measures.

As for the site data, the Spearman correlation coefficients between the deletion rate and substitution measures are significant and positive (Figs. 6 and 7; $P < 0.0001$). However, the strength of correlation depends on the substitution measure used. For both dN and dN/dS, the correlation is strong ($\rho \approx 0.5$), but for dS it is weak ($\rho = 0.14$). These correlations disappear completely in the simulated data (Fig. 7). We conclude that rates of deletion and nonsynonymous substitution per gene are positively correlated.

Discussion

Implications on protein sequence evolution

Our study shows that there is indeed a positive correlation between the probability a codon being deleted and its dN/dS value (Figs. 3–7), indicating similarity in patterns of purifying selection against deletion and amino acid replacement. This can be interpreted as that both replacement and deletion can damage the function of an amino acid residue in the protein, thus reducing the fitness of individuals bearing such mutation. However, this site-wise correlation is weak, on the order of $\rho \approx 0.1$; therefore, it would be difficult to predict one kind of selection from the other. In other words, selection against deletions is not completely consistent with selection against replacement.

We believe that one reason for the weakness of the correlation is the existence of "indifferent DNA" (Graur et al. 2013, 2015). Indifferent DNA refers to sequences that are subject to strong purifying selection against deletions but not substitutions, due to its functionality relies more on the length rather than the exact sequences. For example, it is possible that certain amino acids are required to maintain the spatial relationships between other amino acids in the protein and, therefore,

cannot be deleted, but can be replaced by multiple amino acids with similar biochemical properties. Consistent with this idea, the scatter plot in Fig. 6 shows many genes with low deletion rate and high dN/dS, but few genes with high deletion rate and low dN/dS.

In both the Spearman correlation (Fig. 3) and distribution comparison (Figs. 4) dN also produces a correlation to deletion rates, at a level similar to dN/dS. On the other hand, such correlation is very weak when dS is used, even undistinguishable from simulated data in some cases. If we compare the substitution measures to biological processes, dN/dS is an indicator of selection, dS of mutation, and dN is a combination of both. Thus, it is reasonable to suggest that this correlation between deletion and substitution is largely caused by a similar pattern of selection rather than mutation.

Our study on the correlation between substitutions and indels is the first one that involves genomic protein-coding genes, and includes both site-wise and gene-wise analyses. Using the deletion rate inferred from multiple sequence alignments instead of data on genetic diseases (Miller et al. 2007) made the rate estimation across multiple species rather than human-specific. Alignment-derived deletion rates are also available as long as the genomes of these species are annotated, while disease-derived rates are limited to clinical data and lethal sites are excluded. However, due to alignment errors and partial sequences in some species, alignment-derived deletion rates are less reliable. Nevertheless, we believe that we have taken precautions for these disadvantages, respectively by use of simulation and datasets “4+”/“6+.”

The potential non-independence between selection against substitutions and deletions can also be relevant in studies involving simulated sequence evolution. In protein simulation, the algorithm writer must decide whether to account for this correlation. For example, INDELible, one of the most comprehensive and frequently used simulation programs, does not allow variation of indel rates along the sequence (Fletcher and Yang 2009). On the other hand, programs like SIMPROT (Pang et al. 2005) implements an algorithm that chooses indel positions relative to their substitution rates. ROSE (Stoye et al. 1998) and indel-Seq-Gen (Strope et al. 2009) limit indels to less conserved regions of sequences.

Difference between site-wise and gene-wise analyses

Site-wise and gene-wise analyses on evolutionary parameters often yield different results (e.g., Wang et al. 2013). Here, we have shown that the Spearman correlation between dN, dS as well as dN/dS and deletion rate are more than 4 times higher in gene-wise comparisons (Fig. 7) than in site-wise comparisons (Fig. 3). dN/dS values vary in a much larger range in site-wise than gene-wise analyses (Lindblad-Toh et al. 2011). It is possible for sites (individual amino acids) to undergo positive selection which yields a dN/dS above 1, while this is rare for a whole gene because a protein's basic structure need to be kept consistent for it to function. Therefore, a site-wise study can provide a higher resolution on the selection schemes on the coding part of genomes. On the other hand, site-wise studies suffer from a low sample size for each data point, and thus larger random error.

While the most likely reason for a much higher gene-wise correlation is that the stochasticity of both substitution and indel rates on the site level causes a low

signal-to-noise ratio, it is also possible that between-gene differences contribute more to the overall correlation than within-gene differences. Traditional methods for distinguishing within-category and between-category effects such as ANCOVA are not applicable here due to the non-normal distribution of deletion rates, therefore we looked at the within-gene correlation between deletion rates and substitution measures in individual genes. We conclude that the within-gene effects are smaller than the between-gene effects, as the within-gene Spearman's ρ is smaller than that from the total dataset. On a population genetics level, it is possible that 1) selection is similar within one gene because the deleterious effects of mutations are similar, and 2) mutation rates within one gene (a short region in the genome) do not have much variation.

Artifactual correlation caused by alignment errors

Aside from the biological insights into protein sequence evolution, this study also provides information about consequences of alignment errors. There is no pre-determined correlation between indels and dN/dS in the simulated sequences, thus all estimated correlation is due to artifacts. The correlation between dN/dS and deletion in true alignments of simulated sequences is undistinguishable from zero, which confirmed this point. The same correlations estimated from inferred alignment, on the other hand, are consistently higher than zero. The only difference between them is the presence of alignment error, therefore we can conclude that the small correlation observed in simulated reconstructed alignments is caused by alignment errors.

Multiple sequence alignment is a mathematically difficult (NP-complete) problem; an optimal solution, though theoretically exists, is impossible to implement due to

the time needed is immense. All current multiple sequence alignment algorithms use heuristic methods. These algorithms typically produce alignments that are shorter than the true alignment due to preferring mismatches over gaps, and gives mathematically optimal placements while the real process is sub- or co-optimal (Landan and Graur 2008, 2009). Regions that are rich in insertions and deletions are difficult to align due to co-optimal placement of gaps, thus putting gaps and mismatches together more often than it should be.

On the other hand, there is a correlation between dN and deletion as well as dS and deletion in simulated sequences that cannot be explained by alignment errors. This phenomenon appears in both true and inferred alignments, and in both site-wise and gene-wise analyses. The most likely explanation is different rates of evolution (tree length) among different genes, because dN, dS and deletion rate are all indicators of total evolutionary change along the entire tree.

Phase-1 and Phase-2 deletions

A phase-1 or phase-2 codon deletion (deletions that only partially encompass the first and the last codon involved) can cause an amino acid mismatch without nucleotide substitutions. They are also called non-conservative deletions because they do not conserve the undeleted amino acids (de la Chaux et al. 2007). However, past studies demonstrated that such events are rare. In a study on pairwise indel event between mouse and rat, 12% of indels found are non-conservative, in contrast with a simulation expectation of 29% (Taylor et al. 2004); another study (de la Chaux et al. 2007) gave an even lower estimate that 4% of all deletions are non-conservative from 3-primate alignments.

Unfortunately, with the simulation and alignment methods we used, we could not account for the effects for such deletions, nor could we mimic them by simulation. Nevertheless, the mismatch caused by non-conservative deletions usually does not happen in the same site as the gap. For example, if ACGCAT (Thr-His) became A--AT (Asn), the Asn residue will be aligned into one of the sites, while the gap occupies the other. The elevated dN/dS would thus only occur in the non-gap site. It is possible that the presence of such a mismatch complicates the alignment process and attracts other alignment errors, but we are not able to quantify this effect.

Caveats and future directions

In our study, the simulation part was used as a negative control. In other words, it was used as a baseline when indel rates and dN/dS are independent from each other. We suggest that in future studies, a positive control can be implemented. If a simulation includes a correlation between indel and substitution models (or even perfectly linearly correlated rates), we could see how the results would compare to the real data. After all, even if the input indel and replacement rates are perfectly linear to each other, the site-wise correlation would still not be one because of stochastic effects.

In the phylogenetic tree used in this study, we put the horse (Perissodactyla) and the dog (Carnivora) together as sister groups, while the cow (Cetartiodactyla) is a sister group for the horse+dog clade. This hypothesis, known as Pegasoferae, is supported by a phylogenetic study using molecular data (Nishihara et al. 2006). However, the evolutionary relationship among horse, dog and cow is still under debate. A rival hypothesis groups the horse and the cow together (Perissodactyla +

Cetartiodactyla = Euungulata), to the exclusion of the dog (Prasad et al. 2008). We reasoned that in both hypotheses, the branch separating two of them from the third is very short, and this controversy would have a minimal effect on the estimation of evolutionary parameters. Therefore, we have arbitrarily chosen the Pegasoferae hypothesis. It may be a good idea to check if the choice of phylogenetic tree will affect the result in the future.

Conclusion

This study has demonstrated that in the evolution of mammalian proteins, the selection regimes on amino acid replacement and on short deletions are weakly correlated to each other. Codons that are less likely to undergo nonsynonymous substitutions are statistically also less likely to be deleted. However, in practice this correlation can be overestimated due to the effects of alignment errors.

Materials and Methods

Data collection and analysis of dN, dS and dN/dS

A list of aligned mammalian protein sequences was taken from Lindblad-Toh et al. (2011). To make sure that only good-quality genome sequences were used, we only included data from 9 mammalian species (Fig. 1): human (*Homo sapiens*), chimpanzee (*Pan tryglodytes*), macaque (*Macaca mulatta*), rat (*Rattus norvegicus*), mouse (*Mus musculus*), guinea pig (*Cavia porcellus*), dog (*Canis lupus familiaris*), cow (*Bos taurus*), and horse (*Equus caballus*). We retained 8,605 alignments. Coding DNA sequences that correspond to these sequences were retrieved from ENSEMBL 2011 archive (Flicek et al. 2011).

All protein sequences were aligned with PROBCONS with default parameters (Do et al. 2005), and DNA sequences were threaded through the protein alignments. Maximum likelihood trees were produced with RAxML (Stamatakis 2006) from the alignments, with a GTR+Gamma model and tree topology restricted to that of Fig. 1, and all other parameters set to default (standard hill-climbing algorithm). To reduce bias caused by unrealistic trees, 10 genes that produced a total tree length above 5 were discarded. Throughout the study, we used the remaining 8,595 genes. The DNA alignments were processed through the program HyPhy using the FUBAR script (Murrell et al. 2013), which estimated the dN and dS of each site using an approximate Bayesian algorithm, a Markov chain Monte Carlo process that compares a large number of site classes to identify and estimate selection. Their ratio ω = dN/dS was calculated from the output of FUBAR.

Deletion identification and statistical analysis

Deletions of 1 to 8 amino acids were identified along seven pairs of branches (Fig. 1). These branch pairs are: (a) human and chimpanzee lineages (red branches, macaque as outgroup); (b) ape and macaque lineages (green branches, cow as outgroup); (c) rat and mouse lineages (indigo branches, guinea pig as outgroup); (d) murid and guinea pig lineages (orange branches, human as outgroup); (e) primates and rodents lineages (purple branches, cow as outgroup); (f) dog and horse lineages (yellow branches, cow as outgroup); (g) (dog+horse) and cow lineages (cyan branches, human as outgroup). The outgroup was used to determine whether a gap in the alignment is caused by an insertion or a deletion (Fig. 2A). In branch pair (b), the closest outgroup is a rodent, but cow was chosen because rodents have long branch lengths. For a lineage containing multiple species (e.g.,

apes), only the branch before the divergence (e.g., divergence between human and chimpanzee) was analyzed. This was done by combining multiple sequences into an "ancestral" sequence: any site that is a gap in *all* combined species is a gap site in the "ancestor", and if the site is not a gap in at least one of these sequences, it is considered non-gap in the "ancestor." In this way, every branch in the nine-species tree, excluding the root branch, was searched for deletions without repetition. The root branch (the branch separating the primates-rodents group and other mammals) was not searched for deletions because the directions of its indels could not be determined.

A fraction of amino acid sites are excluded from analysis because of ambiguity and difficulties in detecting deletions or substitutions. These sites include gaps in the outgroup (Fig. 2B), gaps in both ingroup taxa (Fig. 2C), deletions over 8 amino acids long (Fig. 2D), ambiguous amino acids (Fig. 2E), and terminal gaps (Fig. 2F). In some cases we excluded a site in the analysis of one lineage pair but not another.

The deletion rate of an amino acid site, D, is calculated as $D = \frac{\sum_{i=1}^{7} D_i}{\sum_{i=1}^{7}(L_i \times V_i)}$. $D_i = 1$ if that site is part of a deletion in the ith lineage pair, and 0 otherwise; $V_i = 1$ if that site is **not** excluded in that lineage pair, and 0 otherwise; L_i is the sum of branch lengths of the ith lineage pair, based on the placental tree (without chromosome X) from human/hg19/GRCh37 46 species multiple alignment (http://genomewiki.ucsc.edu/index.php/Human/hg19/GRCh37_46-way_multiple_alignment, Kent et al. 2002; Fig. 1).

The deletion rate of a gene, D_G is calculated as $D_G = \frac{\sum_{j=1}^{n}\sum_{i=1}^{7} D_{ij}}{\sum_{j=1}^{n}\sum_{i=1}^{7}(L_{ij} \times V_{ij})}$, where n is the number of codons in the gene, D_{ij} is D_i in the jth codon in that gene, and L_{ij} is L_i in the jth codon in that gene.

For each amino acid site in each alignment, four values were obtained: deletion rate and three substitution measures (dN, dS and dN/dS). For each alignment method, Spearman correlation coefficients were calculated between the weighted deletion rate and the three substitution measures. This dataset uses all sites and is thus named "**All**." See Table 1 for summary statistics on this dataset.

To reduce the effects of spuriously high or low values of dN/dS due to "gappy" sites, the correlation coefficients were recalculated for (1) sites that have not experienced a gap event in at least four sequences, and (2) sites that have not experienced a gap event in at least six sequences. These datasets are referred to as "**4+**" and "**6+**", respectively. Many sites have not experienced any nucleotide substitution, and their dN/dS is technically incalculable due to division by 0, only approximated using extrapolation from other sites. Therefore, we generated sub-datasets in which these constant sites were excluded. These datasets were named "**NC-All**," "**NC-4+**" and "**NC-6+**," where "NC" stands for "no constant."

Coding sequence simulation and analysis

We simulated coding DNA sequences using INDELible (Fletcher and Yang 2009). INDELible evolves nucleotide sequences along the input tree based on a nucleotide substitution model. These substitutions are subject to selection as determined by dN/dS, randomly drawn from an input distribution for each site. Insertions and deletions, always multiples of three nucleotides, are independently modeled and

have a uniform rate among sites; however, the number of indels is proportional to the branch length.

We simulated a total of 8,595 genes × 5 replicates. For each gene, the ancestral gene length and level of divergence were based on the values derived from the corresponding real gene (see Supplementary Text for details). The distribution of dN/dS was a gamma distribution with a shape parameter of $\alpha = 0.5$ (approximated from real data) and a mean calculated from its real data counterpart. The distribution was discretized into 50 bins between 0 and 1 (0–0.02, 0.02–0.04 …), 20 bins between 1 and 2 (1–1.05, 1.05–1.1 …) and 1 bin above 2. In each bin, the dN/dS value used was the median. If a bin (usually the ones with highest dN/dS) has a probability below 10^{-6} in the gamma distribution, it was not used. The absolute deletion rate for each gene was drawn from a gamma distribution with a shape parameter of $\alpha = 0.6$ (approximated from real data) and mean = 0.79 (the mean S_{AI} from the real data), so that it is independent from substitution rate (see Supplementary Text); the relative indel rate was calculated based on absolute indel rate and branch lengths.

The simulated protein sequences were aligned with PROBCONS (alternative alignment tools give identical results), and then nucleotide alignments were threaded through the protein alignments. We estimated deletion rates and substitution measures based on these alignments, as well as for the "true" alignment (as control for alignment error), as described above for real data. See Table 1 for summary statistics on the simulated data.

We used bootstrapping to generate plausible ranges of values of the sequence statistics to compare with the ones obtained from real data. We generated 1,000 bootstrap subsets of the simulated data. In each subset, one random replicate was

chosen from the five for each of the 8,595 genes. Spearman correlation coefficients were calculated for each subset. Each subset was processed as described for real data to generate datasets of each type ("All," "4+," "6+," "NC-All," "NC-4+," and "NC-6+"). For the Spearman correlation coefficients, the mean, standard deviation, and 2.5% and 97.5% quantiles were calculated. We used *Z*-tests to compare the Spearman coefficients derived from real and simulated data.

Distribution of dN/dS in deleted sites

All real mammalian protein sites that have undergone at least one deletion in any lineage were extracted from the data set and their distributions of estimated dN/dS are computed. The distributions were compared with those from deletion-free sites with χ^2 tests. Effect sizes (Cohen's *D*, Cohen 1988) were calculated between dN/dS distributions in deletion and non-deletion codons. These analyses were only done on "All" and "NC-4+" datasets as representative of all six datasets. These procedures were repeated for the simulated data. Similar to the previous section, 1,000 bootstrap subsets were used, and the mean, standard deviation, and 2.5% and 97.5% quantiles were calculated. Z-tests were used to compare real to simulated data.

Analysis of gene-wise correlations

For both real and simulated data, we calculated gene-wise dN, dS, dN/dS and deletion rate. Gene-wise dN and dS are the mean of corresponding values of "4+" sites over the whole gene. We did not use "NC-4+" because excluding substitution-free sites is likely to lead to overestimation of the substitution measures. Gene-wise

dN/dS is gene-wise dN divided by gene-wise dS. The calculation of gene-wise deletion rate is described in a previous sub-section.

We calculated the Spearman correlation between gene-level deletion rate and substitution measures in both real and simulated data, for each alignment method. Similar to previous sections, in the simulated data bootstrapping is used. Each subsample includes only one replicate for every simulated gene. The mean, standard deviation, and 2.5% and 97.5% quantiles were calculated. Z-tests were used to compare real to simulated data.

Acknowledgements

We used the Maxwell cluster from the Center of Advanced Computing and Data Systems (CACDS) at the University of Houston. CACDS staff provided technical support. We would like to thank Sarah Parks and her colleagues at EMBL-European Bioinformatics Institute for their help in running the SLR program on part of our data. R.B.R.A. was funded by NIH R01GM101352. We would also like to thank Jaanus Suurväli and Jan Gravemeyer at University of Cologne for their help in manuscript editing.

References

Cartwright R. (2009) Problems and Solutions for Estimating Indel Rates and Length Distributions. *Mol Biol Evol* 26:473–480.

Chen J-Q, Wu Y, Yang H, Bergelson J, Kreitman M, Tian D. (2009) Variation in the Ratio of Nucleotide Substitution and Indel Rates across Genomes in Mammals and Bacteria. *Mol Biol Evol* 26:1523–1531.

Cohen J. (1988) Statistical Power Analysis for the Behavioral Sciences (second ed.). Lawrence Erlbaum Associates. 67.

de la Chaux N, Messer PW, Arndt PF. (2007) DNA indels in coding regions reveal selective constraints on protein evolution in the human lineage. *BMC Evol Biol* 7:19.

Do CB, Mahabhashyam MSP, Brudno M, Batzoglou S. (2005) ProbCons: Probabilistic consistency-based multiple sequence alignment. ProbCons: Probabilistic consistency-based multiple sequence alignment. *Genome Res* 15:330–340.

Edgar RC, Batzoglou S. (2006) Multiple sequence alignment. *Curr Opin Struc Biol* 16:368–373.

Fletcher W, Yang Z. (2009) INDELible: A Flexible Simulator of Biological Sequence Evolution. *Mol Biol Evol* 26:1879–1888.

Flicek P, Amode MR, Barrell D, Beal K, Brent S, Chen Y, Clapham P, Coates C, Fairley S, Fitzgerald S, et al. (2011) Ensembl 2011. *Nucleic Acids Res* 39:D800–D806.

Graur D. (2016) *Molecular and Genome Evolution*. Sinauer Associates, Sunderland, MA.

Graur D, Zheng Y, Azevedo RBR. (2015) An evolutionary classification of genomic function. *Genome Biol Evol* 7:642–645.

Graur D, Zheng Y, Price N, Azevedo RBR, Zufall RA, Elhaik E. (2013) On the Immortality of Television Sets: "Function" in the Human Genome According to the Evolution-Free Gospel of ENCODE. *Genome Biol Evol* 5:578–590.

Jukes TH, Kimura M. (1984) Evolutionary constraints and the neutral theory. *J Mol Evol* 21:90–92.

Kent WJ, Sugnet CW, Furey TS, Roskin KM, Pringle TH, Zahler AM, Haussler D. (2002) The human genome browser at UCSC. *Genome Res* 12:996–1006.

Landan G, Graur D. (2008) Local reliability measures from sets of co-optimal multiple sequence alignments. *Pac Symp Biocomput* 13:15–24.

Landan G, Graur D. (2009) Characterization of pairwise and multiple sequence alignment errors. *Gene* 441:141–147.

Lindblad-Toh K, Garber M, Zuk O, Lin MF, Parker BJ, Washietl S, Kheradpour P, Ernst J, Jordan G, Mauceli E, et al. (2011) A high-resolution map of human evolutionary constraint using 29 mammals. *Nature* 478: 476–482.

Miller W, Rosenbloom K, Hardison RC, Hou M, Taylor J, Raney B, Burhans R, King DC, Baertsch R, Blankenberg D, et al. (2007) 28-Way vertebrate alignment and conservation track in the UCSC Genome Browser. *Genome Res* 17:1797–1808.

Miyata T, Yasunaga T, Nishida T. (1980) Nucleotide sequence divergence and functional constraint in mRNA evolution. *P Natl Acad Sci USA* 77:7328–7332.

Murrell B, Moola S, Mabona A, Weighill T, Sheward D, Pond SLK, Scheffler K. (2013) FUBAR: A Fast, Unconstrained Bayesian AppRoximation for Inferring Selection. *Mol Biol Evol* 30:1196–1205.

Nagy LG, Kocsubé S, Csanádi Z, Kovács GM, Petkovits T, Vágvölgyi C, Papp T. (2012) Re-mind the gap! Insertion–deletion data reveal neglected phylogenetic potential of the nuclear ribosomal internal transcribed spacer (ITS) of fungi. *PloS One* 7:e49794.

Nei M, Gojobori T. (1986) Simple methods for estimating the numbers of synonymous and nonsynonymous nucleotide substitutions. *Mol Biol Evol* 3:418–426.

Nishihara H, Hasegawa M, Okada N. (2006) Pegasoferae, an unexpected mammalian clade revealed by tracking ancient retroposon insertions. *P Natl Acad Sci USA* 103: 9929–9934.

Pang A, Smith AD, Nuin PAS, Tillier ERM. (2005) SIMPROT: Using an empirically determined indel distribution in simulations of protein evolution. *BMC Bioinformatics* 6:236.

Prasad AB, Allard MW, NISC Comparative Sequencing Program, Green EE. (2008) Confirming the phylogeny of mammals by use of large comparative sequence data sets. *Mol Biol Evol* 25:1795–1808.

Price N, Graur D. (2016) Are Synonymous Sites in Primates and Rodents Functionally Constrained? *J Mol Evol* 82:51–64.

Stamatakis A. (2006) RAxML-VI-HPC: maximum likelihood-based phylogenetic analyses with thousands of taxa and mixed models. *Bioinformatics* 22:2688–2690.

Stoye J, Ever D, Meyer F. (1998) Rose: generating sequence families. *Bioinformatics* 14:157–163.

Strope CL, Abel K, Scott SD, Moriyama EN. (2009) Biological Sequence Simulation for Testing Complex Evolutionary Hypotheses: indel-Seq-Gen Version 2.0. *Mol Biol Evol* 26:2581–2593.

Taylor MS, Ponting CP, Copley RR. (2004) Occurrence and Consequences of Coding Sequence Insertions and Deletions in Mammalian Genomes. *Genome Res* 14:555–566.

Thompson JD, Linard B, Lecompte O, Poch O. (2011) A Comprehensive Benchmark Study of Multiple Sequence Alignment Methods: Current Challenges and Future Perspectives. *PLoS One* 6:e18093.

Wang H, Susko E, Roger AJ. (2013) The Site-Wise Log-Likelihood Score is a Good Predictor of Genes under Positive Selection. *J Mol Evol* 76:280–294.

Waterston RH, Lindblad-Toh K, Birney E, Rogers J, Abril JF, Agarwal P, Agarwala R, Ainscough R, Alexandersson M, An P, et al. (2002) Initial sequencing and comparative analysis of the mouse genome. Nature 420:520–562.

Figure legends

Fig. 1 The commonly accepted phylogenetic relationship among the 9 species used in this study. This tree will be called the external reference tree throughout the paper. Seven different colors denote seven pairs of branches/lineages (A–G) on which deletions were estimated. The black-colored branches are the root of the tree. The branch lengths of the 9-species tree are derived from UCSC Human/hg19/GRCh37 46-way multiple alignment (Kent et al. 2002). These branch lengths are used as guidance for simulation and estimation of deletion rates.

Fig. 2 Illustration of how we identify deletion events and non-used sites in protein sequences for each pair of lineages. **A.** Identified short deletion at sites 3 and 4 in taxon 1. **B.** Excluded sites 3 and 4 because of gaps in the outgroup. **C.** Excluded sites 3 and 4 because both ingroup taxa contain gaps at those positions, thus it is impossible to know whether it is an insertion or a deletion. **D.** Excluded sites 3–12 because of long (> 8aa) deletion. **E.** Excluded sites 2–5 because of unknown amino acids. **F.** Excluded sites 5 and 6 because they are included in a terminal gap.

Fig. 3 Rates of deletion and substitution per site are positively correlated. Spearman correlation between deletion rate and substitution measures (dN/dS, dN and dS) in real and simulated data. **A.** Based on the "All" dataset. **B.** Based on the "NC-4+" dataset, where all sites without any substitutions or present in less than four species were removed. For the simulated data, the value shown is the mean of 1,000 bootstrap replicates, and the error bars are 2.5% to 97.5% quantiles. Real data produces higher correlations than simulated data for all measures.

Fig. 4 Effect size (Cohen's D) indicating the difference of substitution measures (dN/dS, dN and dS) means between deleted and non-deleted sites. **A.** Based on the "All" dataset. **B.** Based on the "NC-4+" dataset, where all sites without any substitutions or present in less than four species were removed. For the simulated data, the shown value is the mean of 1,000 bootstrap re-samplings, and the error bars are 2.5% to 97.5% quantiles.

Fig. 5 Histograms showing dN/dS distribution comparisons between sites with and without deletion, in both **A.** real and **B.** simulated data aligned with PROBCONS. The axis marks the lower bound of each bin, i.e. the bin marked "0" indicates $0 \leqslant dN/dS < 0.1$. It can be observed that the distributions are much more different in real data than in simulated data: the non-deleted sites have a heavier left tail, while the deleted sites have a heavier right tail.

Fig. 6 Gene-wise deletion rates plotted against dN/dS, in both **A.** real and **B.** simulated data. In real data, genes with high dN/dS (right) are more likely to have high deletion rate (up), which is not true in simulated data.

Fig. 7 Gene-wise Spearman correlations between deletion rate and substitution (dN/dS, dN and dS) in real and simulated data. In both dN/dS and dN, the correlation in real data is very high ($\approx$ 0.45) compared to simulated data (<0.05); the difference is much less pronounced in dS. For the simulated data, the shown value is the mean of 1,000 bootstrap re-samplings, and the error bars are 2.5% to 97.5% quantiles.

Supplementary Files

Supplementary File 1. Contains Supplementary Text and Supplementary Figures 1-4.

Supplementary Text: Preliminary rounds of simulations to obtain simulation parameters

Supplementary Figure 1: Flowchart describing the derivation and application of simulation parameters

Supplementary Figure 2: Comparison between reconstructed and true alignment: Spearman correlation between site-wise deletion rate and substitution measures

Supplementary Figure 3: Comparison between reconstructed and true alignment: Cohen's D between substitution measures in deleted and nondeleted sites

Supplementary Figure 4: Comparison between reconstructed and true alignment: Spearman correlation between gene-wise deletion rate and substitution measures

Table 1 A summary of our data, both real and simulated, based on "All" dataset. The Simulated Data was analyzed separately for the PROBCONS realignment and the true alignment.

	Real Data (PROBCONS)	Simulated Data (PROBCONS)	Simulated Data (TRUE)
Number of genes	8,595	42,975	42,975
Total alignment length (aa)	5675396	28458331	28465275
Proportion of constant sites	0.3106	0.2266	0.2275
Number of deletions	50698	338330	340895
Mean deletion size (aa)	1.9591 (1.5845)	1.9218 (1.5434)	1.9274 (1.5412)
Mean site-wise dN (sd)	0.3326 (0.9098)	0.2804 (0.5671)	0.2793 (0.5625)
Mean site-wise dS (sd)	1.9526 (2.6370)	1.5625 (1.8169)	1.5586 (1.8032)
Mean site-wise dN/dS (sd)	0.2687 (0.4891)	0.2705 (0.5630)	0.2705 (0.5654)
Mean site-wise deletion rate (sd)	0.0353 (0.8410)	0.0246 (0.2115)	0.0245 (0.1862)
Mean gene-wise dN (sd)	0.3595 (0.2087)	0.2983 (0.1432)	0.2974 (0.1433)
Mean gene-wise dS (sd)	2.1206 (0.4309)	1.6833 (0.2955)	1.6789 (0.2936)
Mean gene-wise dN/dS (sd)	0.1702 (0.0940)	0.1790 (0.0884)	0.1789 (0.0888)
Mean gene-wise deletion rate (sd)	0.0166 (0.0222)	0.0186 (0.0258)	0.0189 (0.0266)

Fig 1

Click here to download Figure Figure 1.pdf

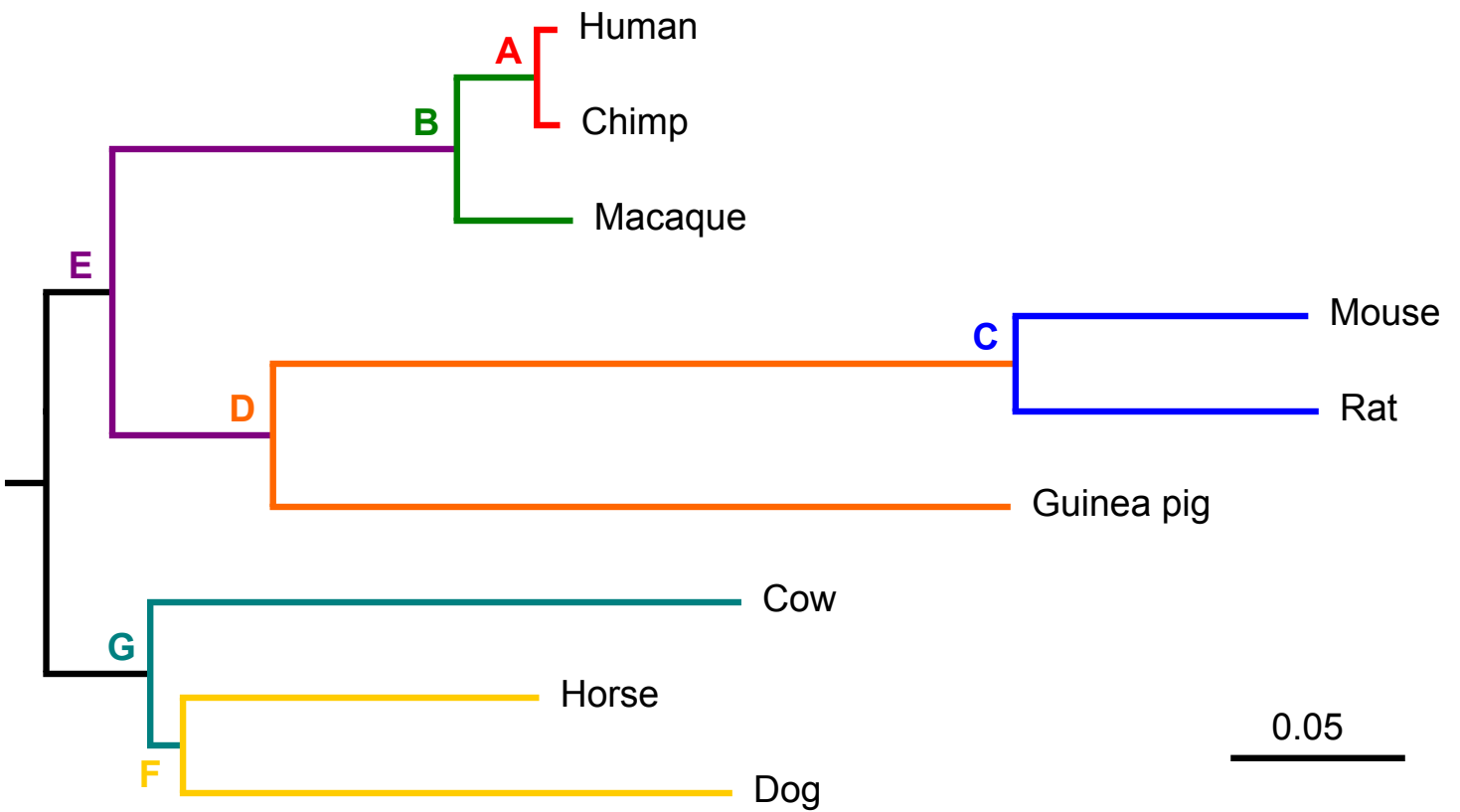

Click here to download Figure Figure 2.pdf

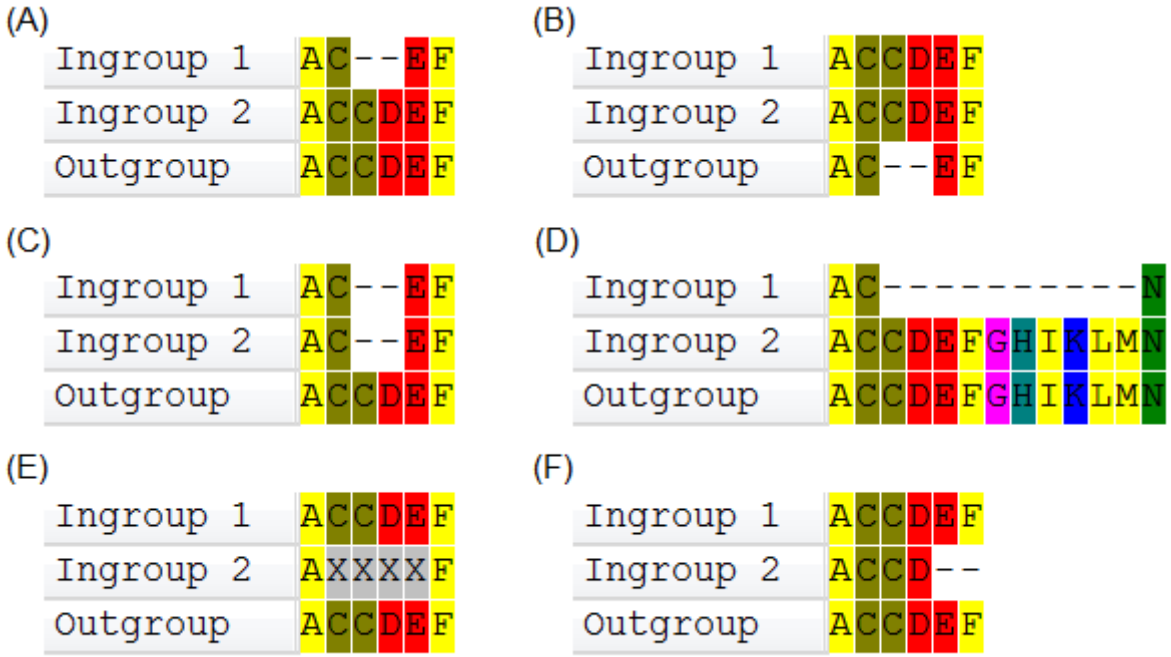

Fig 3

Click here to download Figure Figure 3.pdf

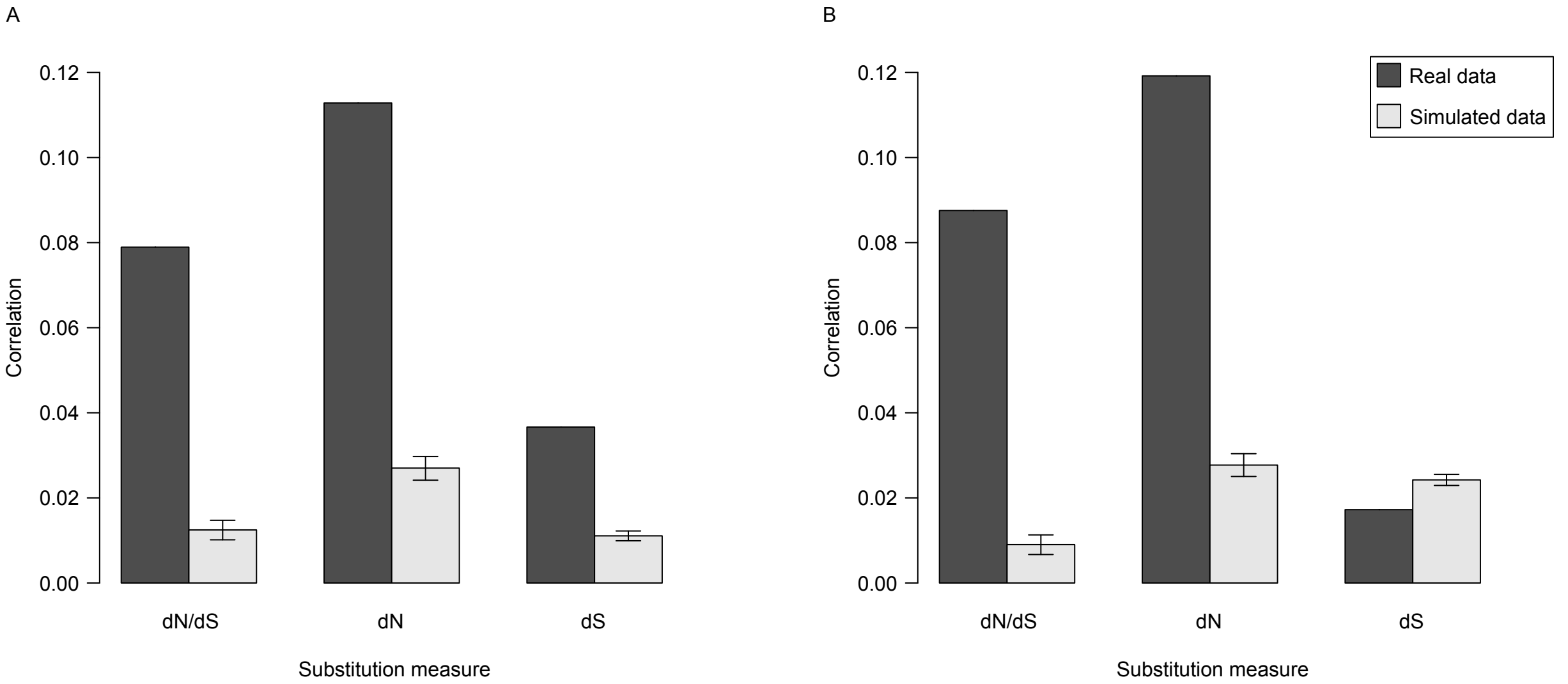

Fig 4

Click here to download Figure Figure 4.pdf

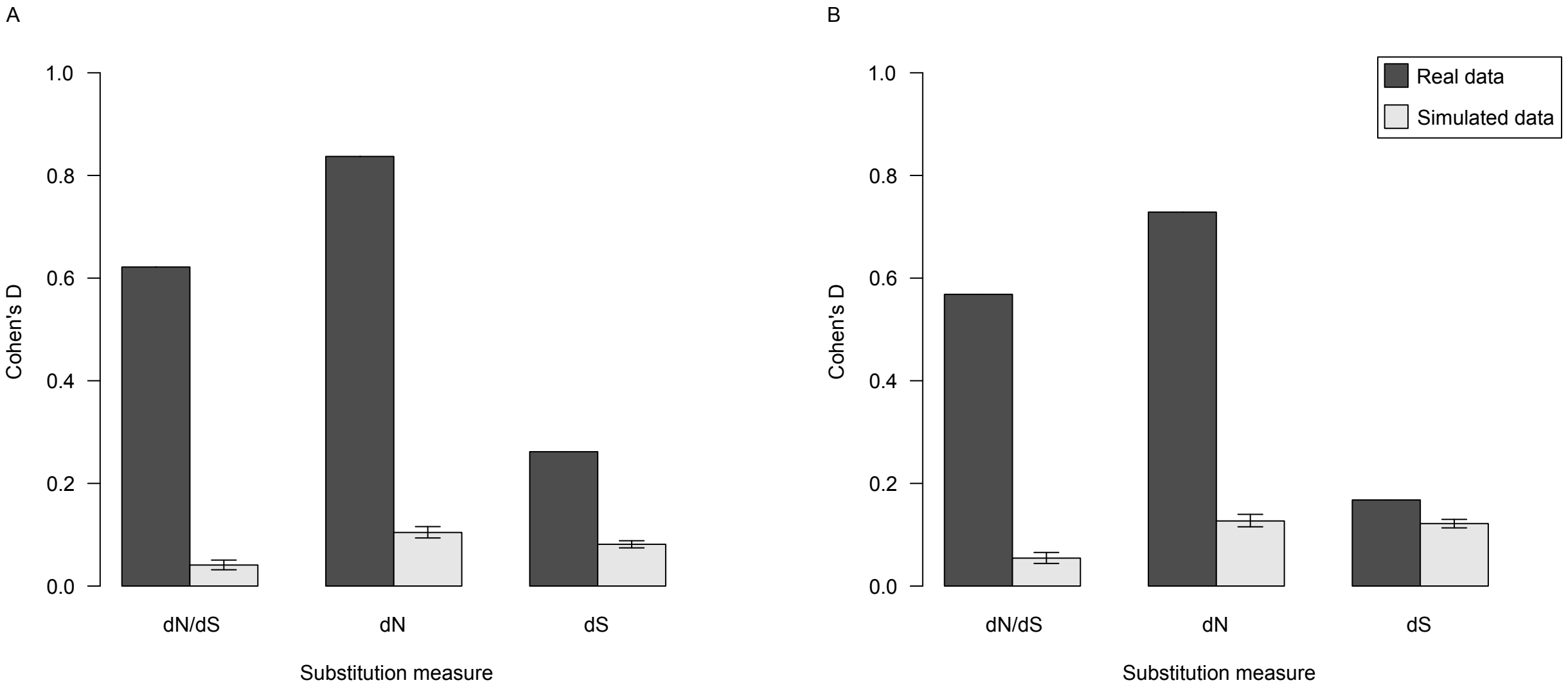

Fig 5

Click here to download Figure Figure 5.pdf

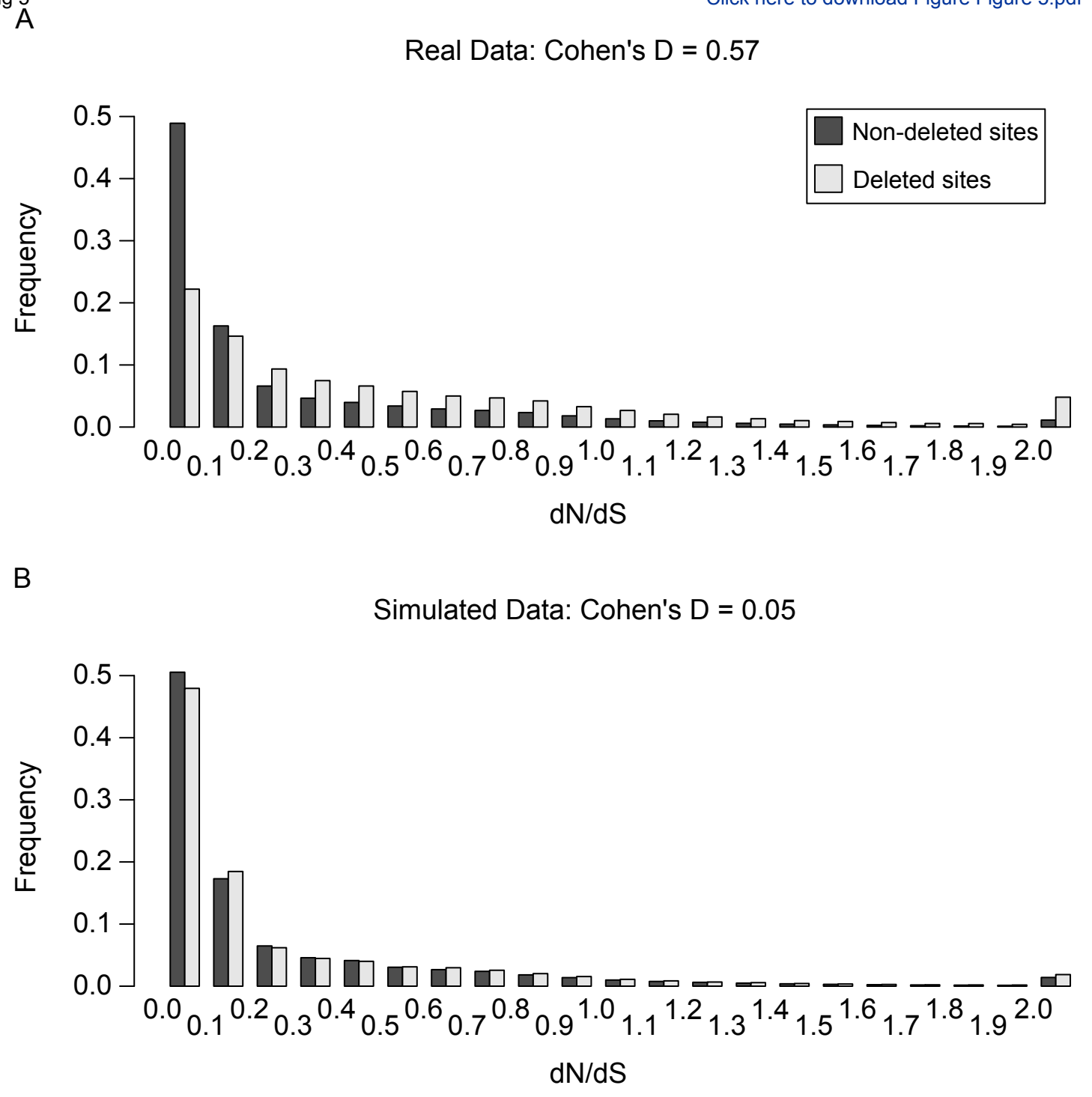

Fig 6

Click here to download Figure Figure 6.pdf

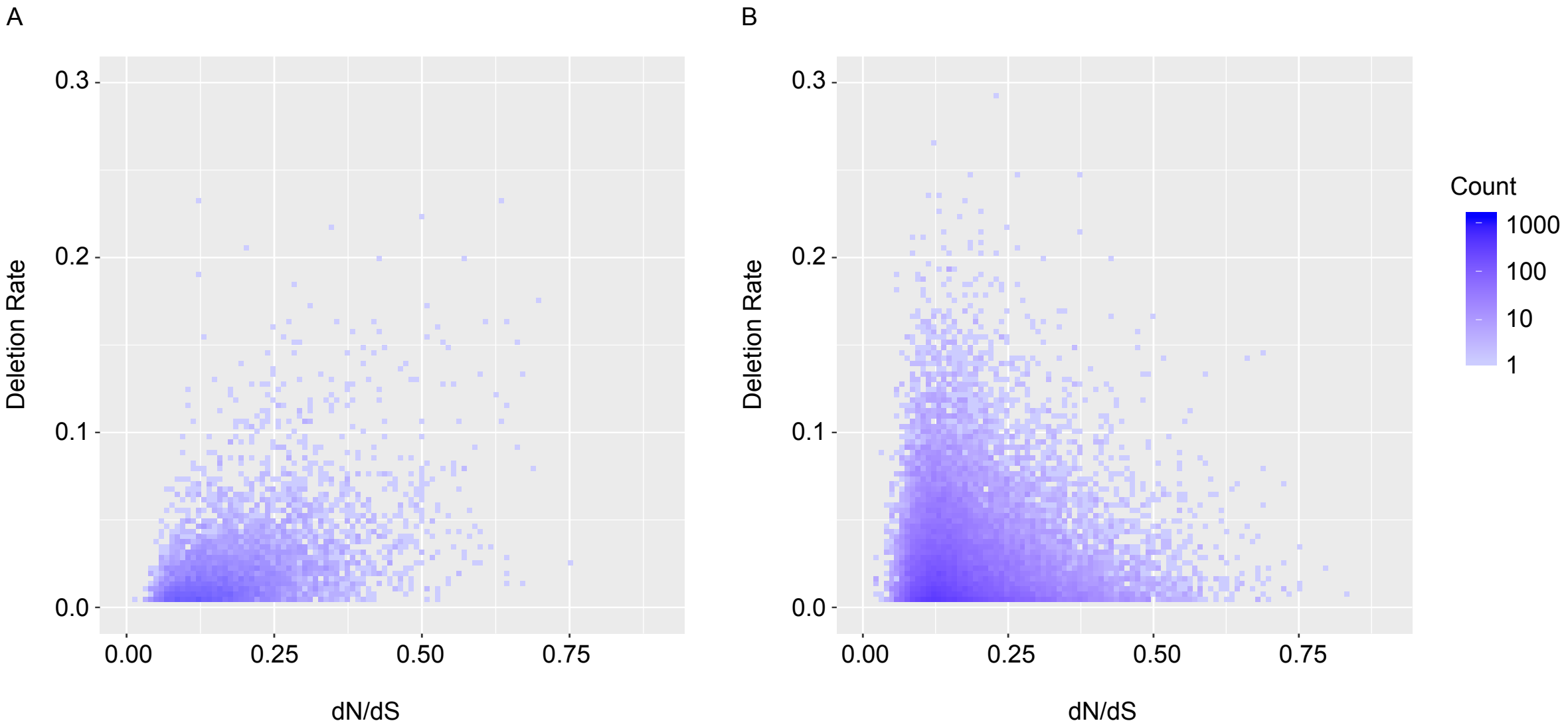

Fig 7
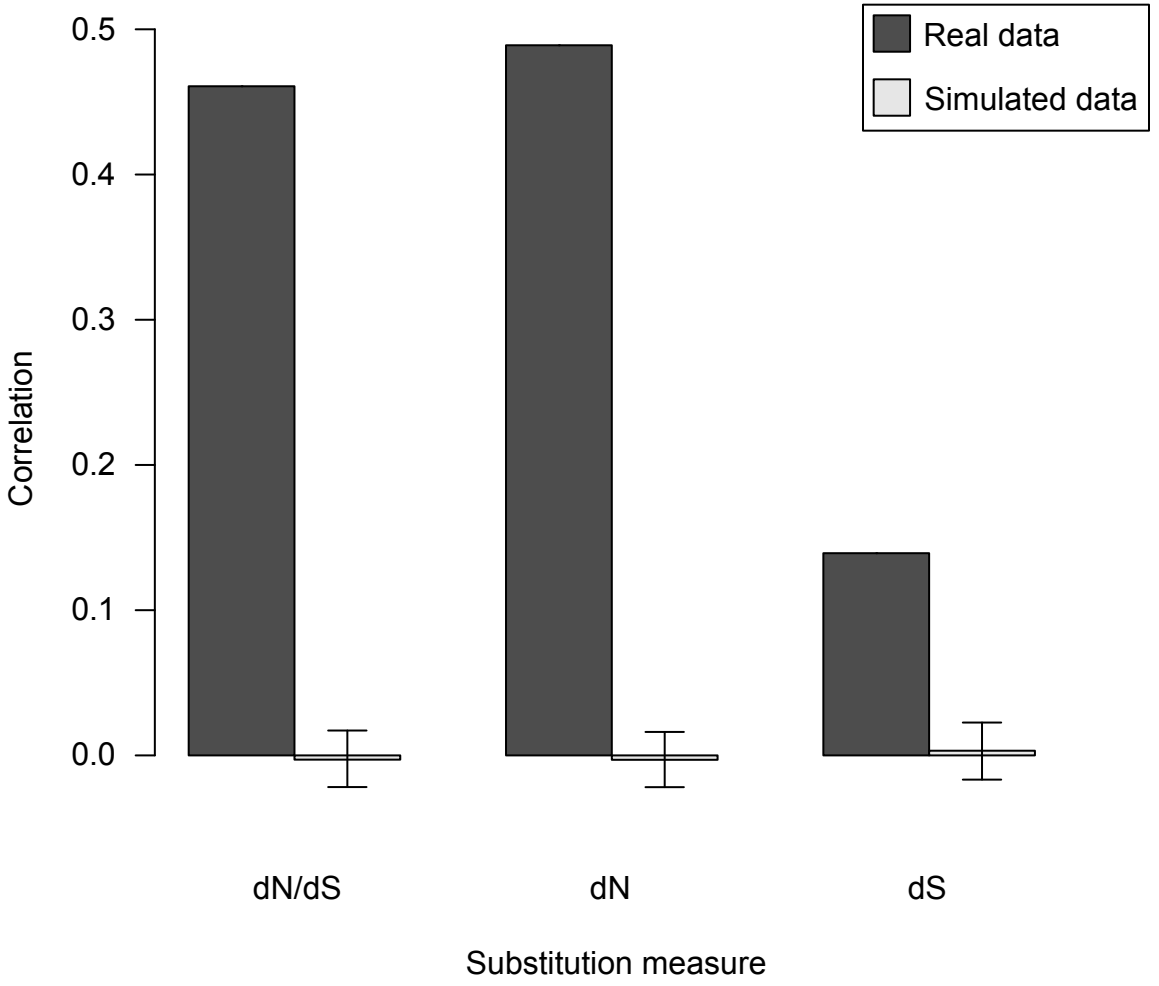
Click here to download Figure Figure 7.pdf